

THE LANDSAT/GLOBAL POSITIONING SYSTEM PROJECT

TERRI WOOD
SYSTEMS DEVELOPMENT BRANCH
GODDARD SPACE FLIGHT CENTER
GREENBELT ROAD, GREENBELT, MD. 20771

ABSTRACT

A GPSPAC/Landsat-D Interface (GLI) Ground Support System was built to validate the performance and to calibrate the accuracy of the experimental navigation package, GPSPAC, flown on the Landsat-4 and 5 spacecraft. Although the GLI system operated successfully to give the orbit information needed to validate the GPSPAC, it also detected two anomalies: one is characteristic of the GLI system and the other is characteristic of the pre-operational phase of GPS. Several methods were applied to resolve or reduce the anomalies. This paper presents a description of the problems, the methods applied to resolve or reduce them, and the results.

2.0 GLOBAL POSITIONING SYSTEM BACKGROUND

The Global Positioning System (GPS) is an advanced satellite-based navigation system, being deployed by the Department of Defense, that will provide extremely accurate position, velocity, and time information to a variety of users 24 hours a day, 7 days a week. Both the Landsat-4 and 5 spacecraft carried an experimental navigation package, the Global Positioning System Package (GPSPAC), to assess the performance and the accuracy of the onboard use of GPS data.

The GPS configuration consists of a Master Control Station (MCS) and a constellation of Navigation Development Satellites (NDSs). In its operational configuration, the NDS constellation will consist of 18 Space Vehicles (SVs) in six nearly circular orbits of 12-hour periods (20,200 km altitude) each inclined 55 degrees to the equator. However, when Landsat-5 was launched in March 1984, the NDS constellation consisted of five operating SVs in two orbit planes with ascending nodes at 120 and 240 degrees, respectively.

The navigation process of GPS proceeds as follows: First, the MCS uplinks messages, consisting of time synchronization and SV ephemeris information, to the NDSs and the NDSs, in turn, continuously broadcast these messages to the user spacecraft. Subsequently, the GPSPAC Receiver/Processor Assembly (R/PA), which is the principle GPSPAC subsystem, records and uses the information onboard and processes pseudorange and delta-pseudorange observations with an Extended Kalman Filter (EKF) to calculate an estimate of the user spacecraft's orbit. (This information is retained to be analyzed and compared with the Landsat definitive ephemeris tape files which are derived from independent sources). If no SVs are in view of the user spacecraft, the R/PA of the user spacecraft must propagate its own orbit by using a numerical integrator.

One aspect of the GPSPAC experiment was to validate and to calibrate the accuracy of the orbit information produced by GPS data; another aspect of the GPSPAC experiment was to determine ways to improve the GPSPAC Kalman Filter's navigation performance by investigating various data base constant changes or by adopting algorithmic changes to the GPSPAC software. To support these efforts, a ground-support-modular system called the GPSPAC/Landsat-D Interface (GLI) System was developed in March 1982 by GSFC's Systems Development Branch. The GLI system consists of five subsystems and the function of each subsystem is described below.

First, the GPSPAC Experiment Data Preprocessor (GEDAP) is the front-end of the system; it reads, sorts, and reformats telemetry strip tape files containing raw GPSPAC measurement data (observations and residuals) and GPSPAC Kalman Filter parameter estimates. Second, the COMPAR subsystem compares ephemeris files from different sources. Next, the PLOT subsystem generates graphs of observations, residuals, and filter parameter estimates as well as ephemeris differences from COMPARE. Finally, the last two subsystems, RECON and ONPAC, are used sequentially. RECON recombines files from GEDAP output to produce data in a form ready for ONPAC to use. ONPAC, the onboard navigation package, is a menu-driven system which has two functions: (1) It uses the recombined files generated from RECON to produce estimates of the GPSPAC navigation solutions by emulating the GPSPAC Kalman Filter data processing scheme. (2) It simulates estimates of the GPSPAC navigation solutions by allowing the user to change various filter parameters; therefore, one can analyze the effect on the GPSPAC navigation solutions once the options are invoked.

The telemetry strip tape files and the Landsat definitive ephemeris tape files, which the GLI system processes, are provided by the Landsat Operations Control Center and by the Ground Spaceflight Tracking and Data Network (GSTDN) Center, respectively. The Landsat Operations Control Center, located at GSFC Building 28, retrieves the telemetry strip tape information from the playback recordings of the GPSPAC during the satellite flyby of a ground tracking station. The GSTDN center, located at GSFC Building 25, collects Unified S-Band (USB) range and range-rate data. Then, the Goddard Trajectory Determination System (GTDS) is used to process the GSTDN USB data and to compute the definitive orbits by performing batch-least squares orbit fits.

3.0 ONPAC AND GPSPAC ANOMALIES

From March 1982 until August 1986, the GLI system was operated successfully to give the orbit information needed to validate the GPSPAC. Namely, comparisons with definitive ephemeris indicated that errors in Landsat-4 and 5 position and velocity from GPSPAC were consistently less than 50 meters and 6 cm/sec, respectively, during periods of good NDS SV visibility (generally speaking 4 SVs in view), and that the peak position errors were generally less than 1,500 meters during periods of poor SV visibility. Although the GLI system helped us to assess the validity of the GPSPAC, it has also enabled us to detect two anomalies: one pertains to the GLI system and the other pertains to the pre-operational phase of GPS. A description of these anomalies is given in the next subsections.

3.1 The ONPAC Anomaly

A problem which pertains to the ONPAC system is depicted by the graphs of the ONPAC position (velocity) uncertainty parameters; these graphs are inconsistent with the graphs of the GPSPAC position (velocity) uncertainty parameters. For instance, figures 1 and 2 illustrate the inconsistencies between the two position uncertainty parameters where each graph was generated during the same arbitrary time span. These inconsistencies suggest that possibly the ONPAC orbit propagator does not match the models of GPSPAC entirely. To understand why the ONPAC position uncertainty parameters graphs differ from the GPSPAC position uncertainty parameters graphs, the ONPAC position differences graphs were analyzed; to resolve the ONPAC inconsistencies, the ONPAC software was investigated and modified. Briefly, the steps taken to resolve the ONPAC inconsistencies involved comparing the GPSPAC navigation code against the supposedly equivalent ONPAC code, modifying the non-conforming routines, and comparing hand-calculated values of various filter parameters (based on the GPSPAC algorithms) with the values used by ONPAC. A detailed explanation of these methods is given in section 4.1.

3.2 The GPSPAC Anomaly

A problem which is characteristic of the pre-operational phase of GPS, is that the GPSPAC/GSTDN definitive position (velocity) differences tend to fluctuate tremendously, when the user spacecraft is forced to propagate its own orbit because of poor SV visibility. For instance, figure 3 illustrates a typical graph of the GPSPAC/GSTDN definitive position difference fluctuations. Also, Figure 4 shows the NDS visibility to the Landsat-4 spacecraft for that period (only NDS SV numbers 5,6,8 & 9 were operational for that period). Notice how the GPSPAC/GSTDN definitive position differences graph peaks whenever there are less than two SVs in view during any particular time span. These fluctuations suggest that there could have been some inconsistencies between the way that the GPSPAC orbit propagator was designed and implemented. Therefore, to investigate this suggestion fully, the GPSPAC navigation software design was compared and analyzed with the software code. In addition to this, ONPAC was used to simulate runs of the GPSPAC definitive position difference fluctuations which enabled us to recommend ways to reduce the actual GPSPAC fluctuations. Briefly, the steps taken to reduce the simulated GPSPAC fluctuations involved studying the GPSPAC navigation design, comparing the design with the actual code (to see if the formulas were implemented correctly), documenting the differences, and changing various ONPAC filter parameters. A detailed explanation of these methods is given in section 4.2.

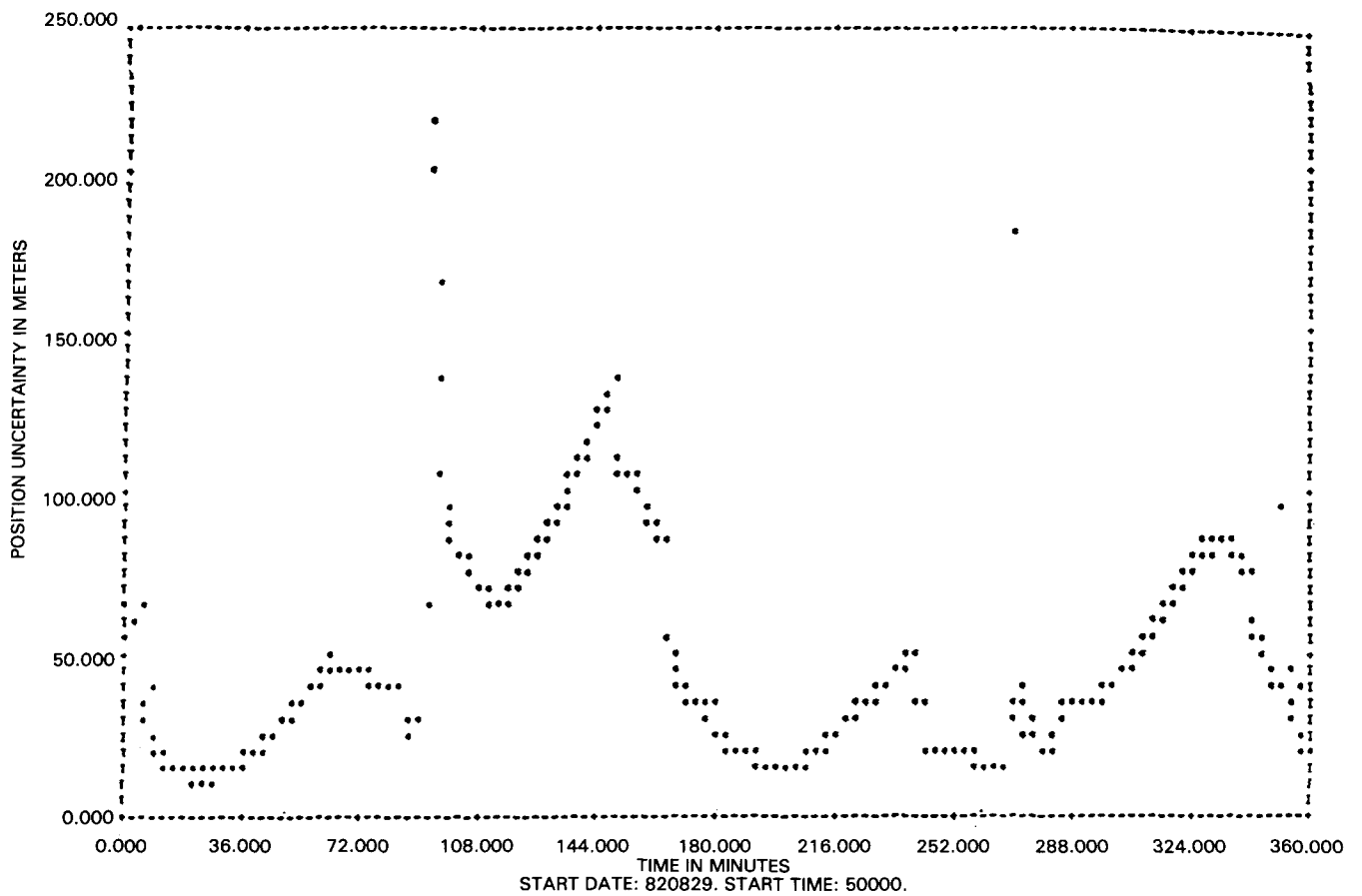


Figure 1. ONPAC Position Uncertainty Parameters

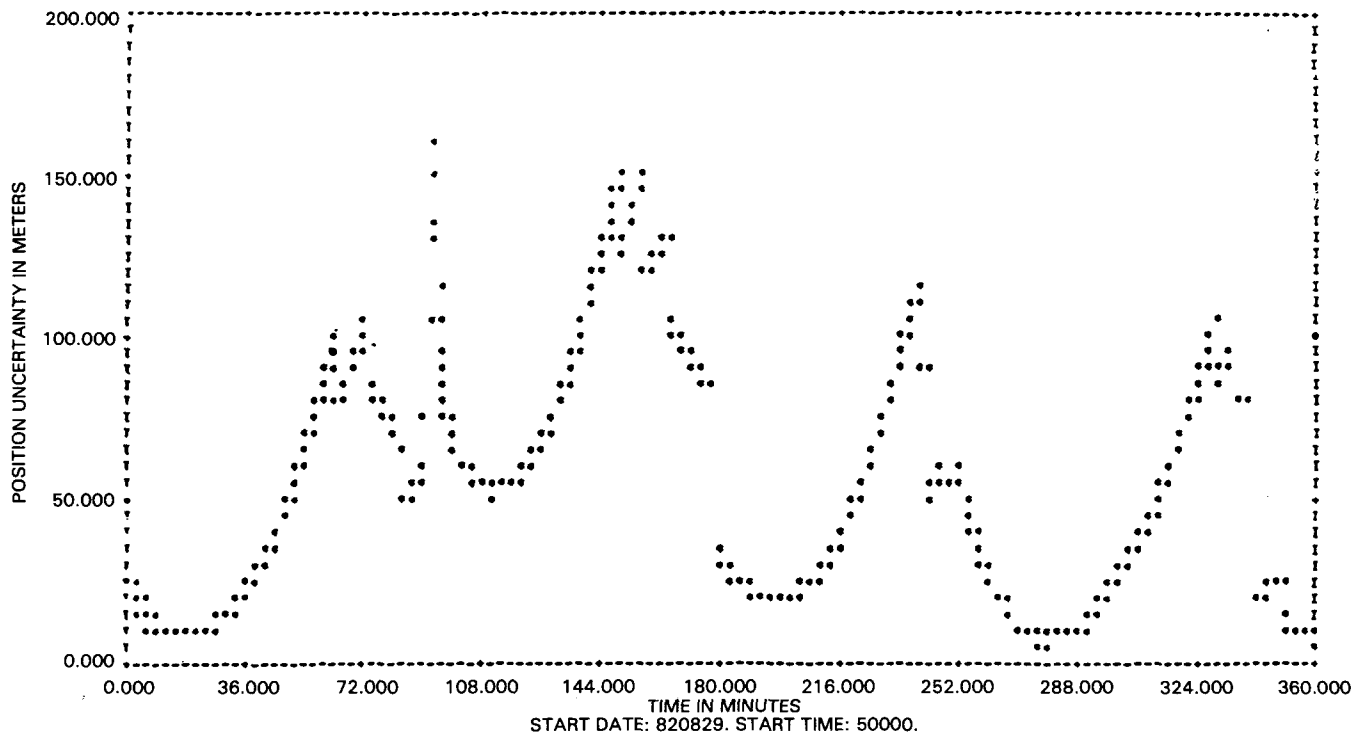


Figure 2. GPSPAC Position Uncertainty Parameters

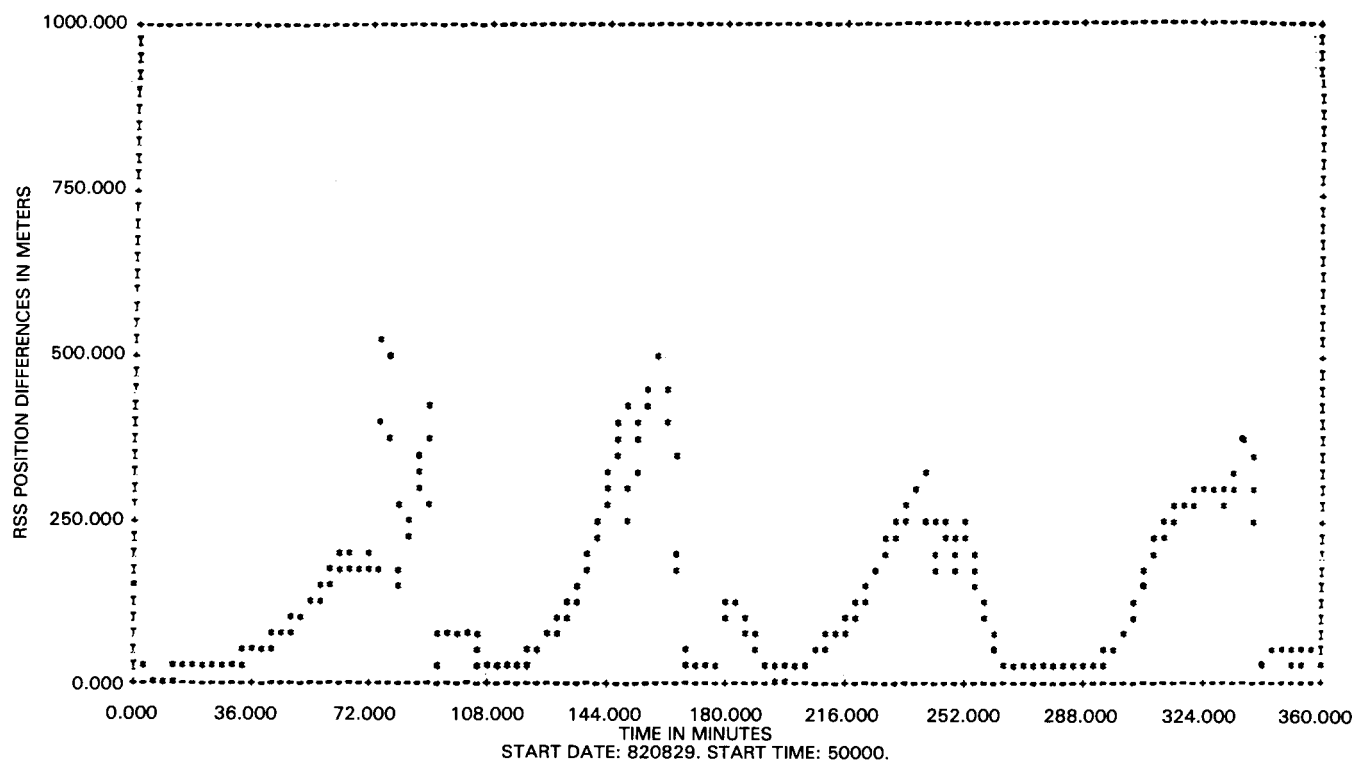


Figure 3. GPSPAC/GSTDN Definitive Position Difference Fluctuations

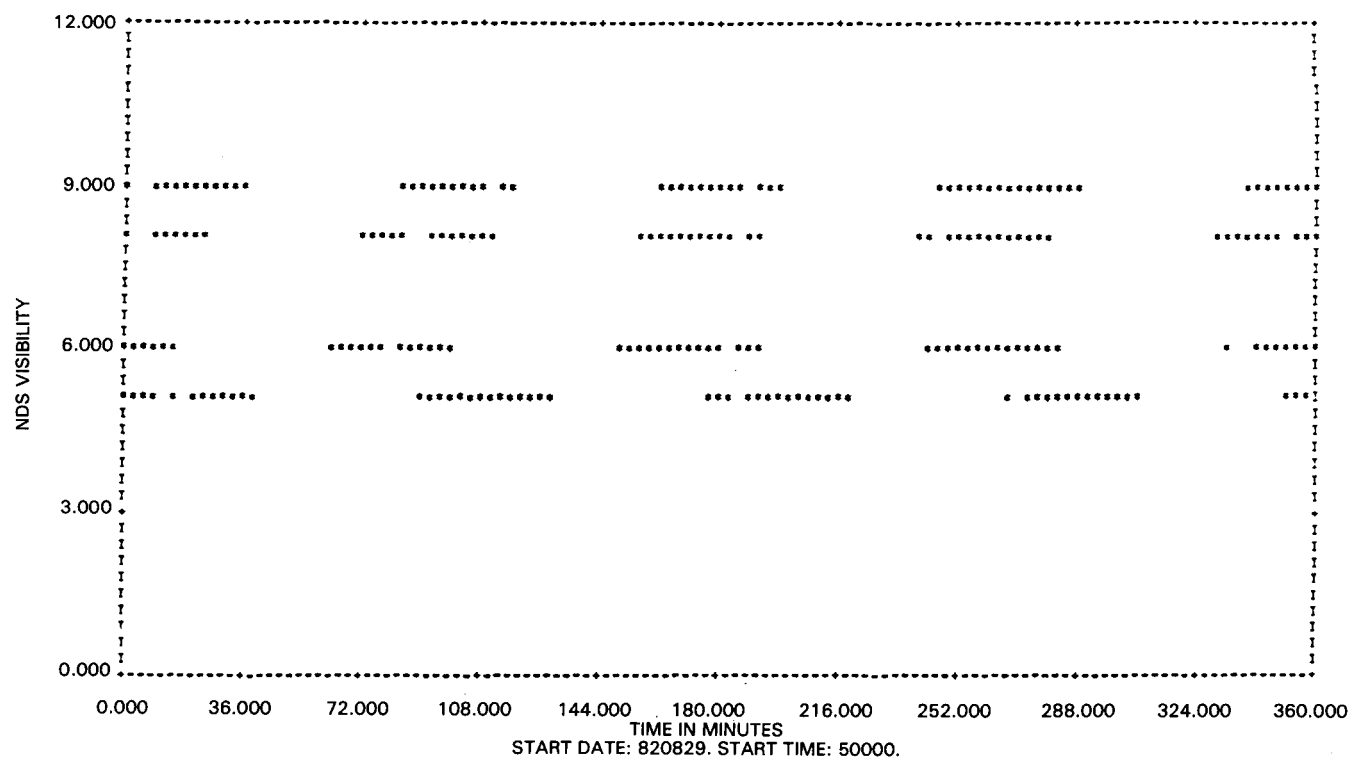


Figure 4. NDS Visibility to Landsat-4

4.0 STEPS TAKEN TO RESOLVE/REDUCE THE ANOMALIES

4.1 Steps Taken to Resolve the ONPAC Anomaly

Since the ONPAC orbit propagator did not match the orbit propagation model of GPSPAC entirely, the ONPAC software was compared with the GPSPAC software to see where the differences occurred. Moreover, several of the filter parameters were calculated by hand to check the computed answers given by ONPAC. A brief description of the GPSPAC/ONPAC code differences, the filter parameters calculated, and the implications of the changes is given in the next subsections.

The GPSPAC/ONPAC Code Differences

The GPSPAC/ONPAC code differences that were found by comparing the two software systems were minor and the following modifications were made to the ONPAC code: First, the geopotential force model in ONPAC, which is one of the modeled external forces used to describe the equations of motion for orbit propagation, was upgraded from a 4x4 earth geopotential model to a 5x5 earth geopotential model to match that of GPSPAC. Next, the atmospheric density model in ONPAC, which is used to model the external drag force (another external force used in orbit propagation), was assigned the same lowest altitude threshold value as that of GPSPAC. Finally, a variable used in ONPAC to validate the pseudorange observations, was replaced with another variable to help simulate the measurement error computation better.

The Filter Parameters Calculated

Another vehicle used to help locate the GPSPAC/ONPAC code differences was to calculate by hand the following EKF parameters given the GPSPAC EKF software, an arbitrary state vector, and the corresponding state-error covariance matrix (see the heading entitled "The EKF Background" for a detailed explanation of these EKF parameters): (1) The arbitrary state vector and the state-error covariance matrix were propagated to the pseudorange measurement time. (2) The pseudorange measurement residual and Kalman Gain were calculated. (3) The state vector was updated by

ORIGINAL PAGE IS
OF POOR QUALITY

adding the Kalman update to it. These hand calculations were done for at least 2 distinctive pseudorange cycles.

The Implications of the Steps Taken to Resolve the ONPAC Inconsistencies

When the ONPAC software code was modified to emulate the GPSPAC propagation model better, the modified ONPAC code was executed, using the same data as before, to generate a better graph of the ONPAC position uncertainty parameters. However, the second graph shows more inconsistencies with the graph of the GPSPAC position uncertainty parameters as did the first graph which was generated using the original ONPAC code (refer to figures 1, 2, and 5 for the comparison). And, to make matters even worse, all of the answers generated from the hand calculations discussed earlier, agreed with the computed answers given by the revised version of the ONPAC software. Consequently, neither of the steps taken to resolve the ONPAC inconsistencies helped; but, it turns out that a method used to reduce the simulated GPSPAC fluctuations also reduces the ONPAC inconsistencies as well and a description of this method is given in the next subsection.

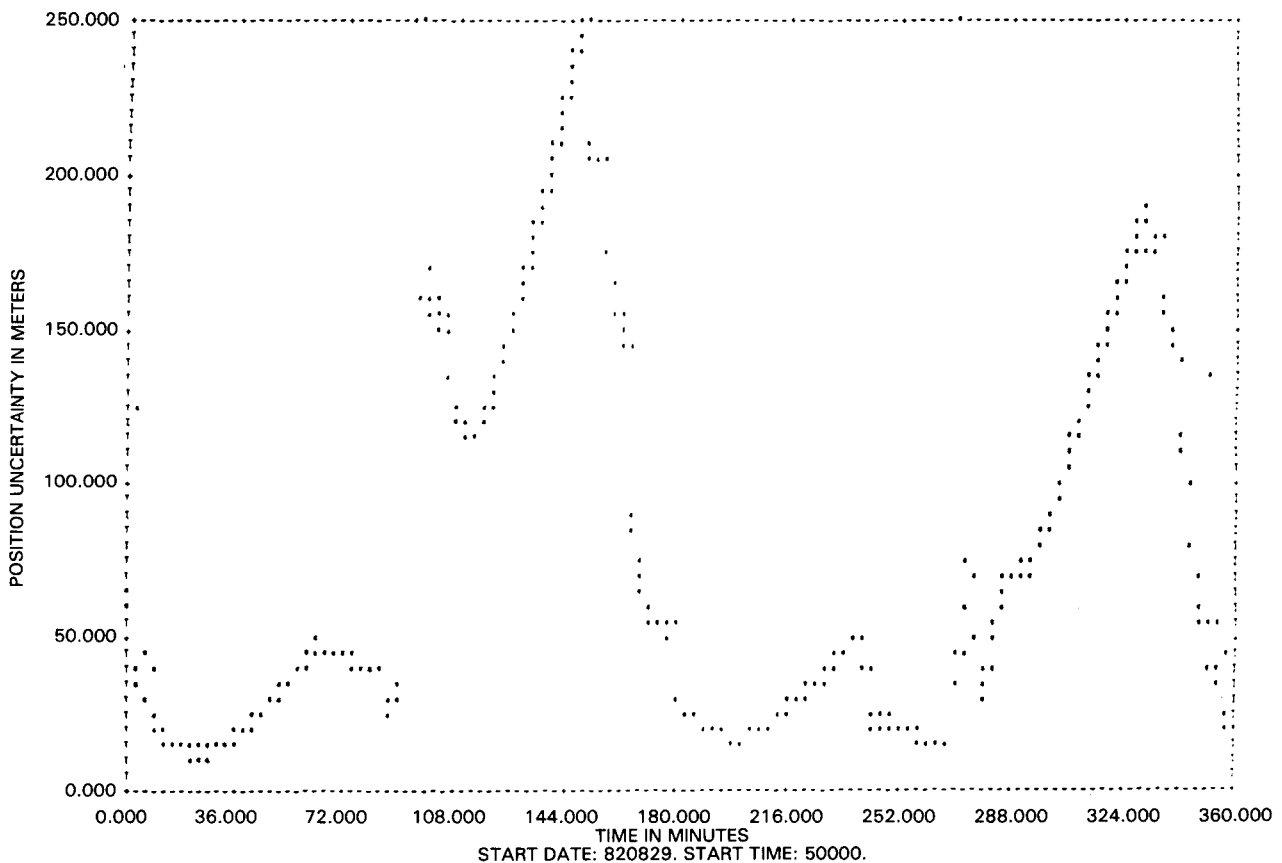


Figure 5. ONPAC Position Uncertainty Parameters using the modified code

4.2 Steps Taken to Reduce the Simulated GPSPAC Anomaly

In order to find out why the GPSPAC fluctuations were occurring, the design of the GPSPAC software and the actual software code were compared to see if there were any inconsistencies between the way the navigation scheme was designed and implemented. Basically, this involved studying the EKF algorithms to see how the navigation solution was propagated and estimated. In order to reduce the simulated GPSPAC fluctuations, various filter parameter changes were invoked using ONPAC. What follows in the next subsections is a description of the EKF (the source of the design-code differences), the results of filter parameter changes, and the implications of these steps taken to reduce the simulated GPSPAC fluctuations.

The GPSPAC Design-Code Differences

The Extended Kalman Filter Background

The Extended Kalman Filter (EKF) is the essential element of the GPSPAC navigation software. The EKF is an algorithm that computes an optimal estimate of the state of a non-linear system, given measurements, initial conditions, and statistical parameters. The filtering algorithm requires two input parameters: an estimate of the state at a previous measurement time and an estimate of the state-error covariance matrix at a previous measurement time. Given the input parameters, the filtering process proceeds as follows:

- (1) The previous filter state, defined as a 9-state vector where components 1-3 and 5-7 are the current position and velocity of the state and components 4, 8, and 9 are the user spacecraft's receiver clock time bias, receiver clock frequency bias, and satellite drag factor, respectively, is propagated to the pseudorange measurement time (distance from the NDS satellite to the user spacecraft divided by the speed of light uncorrected for user clock error).
- (2) The previous filter state-error covariance matrix, defined as a 9x9 matrix where the filter state error is given on the main diagonal, is propagated to the pseudorange measurement time.

- (3) The pseudorange measurement gain is calculated to determine how much can be "gained" from the measurement; then the measurement residual is used to determine an estimate of the state error at the pseudorange measurement time.
- (4) The delta-pseudorange measurement (the difference between two pseudorange measurements) gain is calculated and the measurement residual is used to update the state error estimate of step 3.
- (5) The updated state error estimate is used to correct the propagated filter state from step 1 and the measurement gain calculated is used to update the propagated filter state-error covariance matrix from step 2. This results in a new filter state and a new state-error covariance matrix applicable at the pseudorange measurement time.

Uyeminami describes the EKF process in detail (2).

Figure 6 illustrates the five steps of the filtering process.

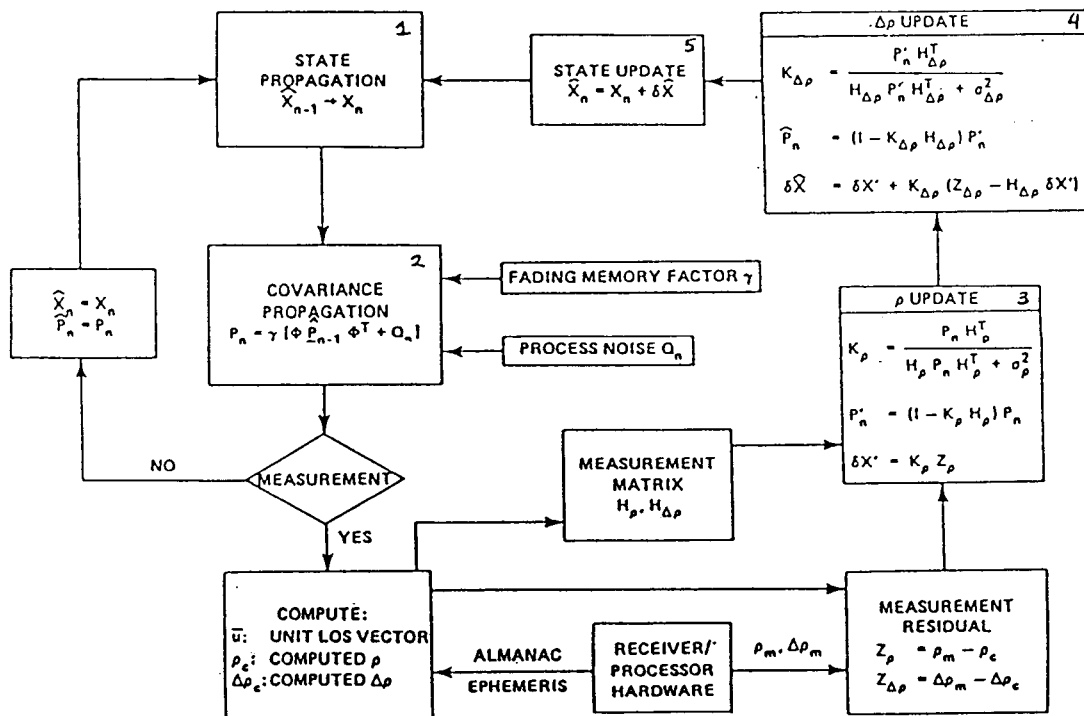


Figure 6. R/PA Extended Kalman Filter

The Source of the Design-Code Differences The State-Error Covariance Matrix

The major design-code differences that were found pertained to the implemented state-error covariance matrix, P_n . The state-error covariance matrix at the current measurement time is computed as: $P_n = \gamma [\Phi \hat{P}_{n-1} \Phi^T + Q_n]$. Briefly, the state transition matrix, Φ , propagates the state-error covariance matrix forward in time and the state-process-noise covariance matrix, Q_n , is computed to compensate for the neglected terms in the force model of the state. See the Mathematical Specifications of the Onboard Navigation Package (ONPAC) Simulator for a detailed description of the state-error covariance matrix derivation (3).

Now, the only way to verify that the software was computing the elements of the state-error covariance matrix exactly the way the design plans had specified was to check and see if the code was computing the elements of the component matrices properly--namely, Φ and Q_n . So, we inspected the equations in the software for both the Φ and Q_n matrices and computed, by hand, the 81 elements in each matrix; as a result, we discovered that the design plan was inconsistent with the code for both matrices.

The Φ Matrix Design-Code Differences

Nine elements near the bottom left-hand side of the Φ matrix pertain to the modeled geopotential acceleration; these elements appeared in the design plans of the matrix, yet, for reasons unknown, they were not computed in the GPSPAC software code (see figure 7). Consequently, the equations of acceleration due to the geopotential were not modeled in the GPSPAC software's version of the estimated corrections to the state.

The Q_n Matrix Design-Code Differences

The design plans for the Q_n matrix is the following:

$$Q_n = \begin{bmatrix} Q_{11} & Q_{12} & Q_{13} \\ Q_{12}^T & Q_{22} & Q_{23} \\ Q_{13}^T & Q_{23}^T & Q_{33} \end{bmatrix}$$

Q_{11} Q_{12} Q_{13}
 Q_{12}^T Q_{22} Q_{23}
 Q_{13}^T Q_{23}^T Q_{33}

	x	y	z	b_{slc}	\dot{x}	\dot{y}	\dot{z}	\dot{b}_{slc}	\dot{d}_{slc}
1	0	0	0	Δt	0	0	0	0	$-\frac{1}{2} \rho_n v_n \Delta t^2 \dot{z}_n$
0	1	0	0	0	Δt	0	0	0	$-\frac{1}{2} \rho_n v_n \Delta t^2 \dot{y}_n$
0	0	0	1	0	0	0	Δt	0	$-\frac{1}{2} \rho_n v_n \Delta t^2 \dot{x}_n$
0	0	0	0	0	0	0	0	Δt	0
$-\frac{\mu}{3} \left(1 - 3 \frac{x_n^2}{r_n^2} \right) \frac{\Delta t}{r_n^3}$	$\frac{x_n}{r_n^3} \frac{\Delta t}{r_n}$	$\frac{x_n y_n}{r_n^5} \frac{\Delta t}{r_n}$	$\frac{x_n z_n}{r_n^5} \frac{\Delta t}{r_n}$	$\frac{x_n^2 + y_n^2 + z_n^2}{r_n^5} \frac{\Delta t}{r_n}$	0	$-\left(\frac{d\phi}{v} \right)_n \frac{\dot{x}_n \dot{y}_n \Delta t}{r_n^2 + \dot{y}_n^2 \Delta t + 2 \dot{z}_n \Delta t}$	$-\left(\frac{d\phi}{v} \right)_n \frac{\dot{x}_n \dot{z}_n \Delta t}{r_n^2 + \dot{z}_n^2 \Delta t}$	0	$-\rho_n v_n \Delta t \dot{x}_n$
$\frac{y_n}{r_n^3} \frac{\Delta t}{r_n}$	$-\frac{\mu}{r_n^3} \left(1 - 3 \frac{y_n^2}{r_n^2} \right) \frac{\Delta t}{r_n}$	$\frac{y_n}{r_n^3} \frac{\Delta t}{r_n}$	$-\left(\frac{d\phi}{v} \right)_n \frac{\dot{y}_n \dot{x}_n \Delta t}{-2 \dot{z}_n \Delta t}$	$-\left(\frac{d\phi}{v} \right)_n \frac{\dot{y}_n^2 + \dot{z}_n^2 \Delta t}{r_n^2 + \dot{y}_n^2 \Delta t + 2 \dot{z}_n \Delta t}$	0	$-\left(\frac{d\phi}{v} \right)_n \frac{\dot{y}_n \dot{z}_n \Delta t}{r_n^2 + \dot{z}_n^2 \Delta t}$	0	0	$-\rho_n v_n \Delta t \dot{y}_n$
$\frac{z_n}{r_n^3} \frac{\Delta t}{r_n}$	$\frac{z_n y_n}{r_n^5} \frac{\Delta t}{r_n}$	$\frac{z_n x_n}{r_n^5} \frac{\Delta t}{r_n}$	$-\frac{\mu}{r_n^3} \left(1 - 3 \frac{z_n^2}{r_n^2} \right) \frac{\Delta t}{r_n}$	$-\left(\frac{d\phi}{v} \right)_n \frac{\dot{z}_n \dot{x}_n \Delta t}{r_n^2 + \dot{z}_n^2 \Delta t}$	0	$-\left(\frac{d\phi}{v} \right)_n \frac{\dot{z}_n \dot{y}_n \Delta t}{r_n^2 + \dot{z}_n^2 \Delta t}$	$-\left(\frac{d\phi}{v} \right)_n \frac{\dot{z}_n^2 + \dot{x}_n^2 \Delta t}{r_n^2 + \dot{z}_n^2 \Delta t}$	0	$-\rho_n v_n \Delta t \dot{z}_n$
0	0	0	0	0	0	0	0	$1 - \frac{\Delta t}{T_F}$	0
0	0	0	0	0	0	0	0	0	$1 - \frac{\Delta t}{T_D}$

Geopotential
Acceleration
Elements \uparrow

Figure 7. State Transition Matrix Φ

where the submatrices Q_{ij} are defined by equations below and elements not indicated in Q_{ij} are taken to be zero.

$$Q_{11} = \frac{1}{4} \sigma_a^2 \Delta t^4 I + \frac{1}{20} \rho_n^2 v_n^2 \sigma_d^2 \Delta t^5 \dot{\underline{r}}_n \dot{\underline{r}}_n^T$$

$$Q_{12} = \frac{1}{2} \sigma_a^2 \Delta t^3 I - \frac{1}{4} \sigma_a^2 \Delta t^4 (2\underline{\Omega} \times I)^T + \alpha_n (v_n^2 I + \dot{\underline{r}}_n \dot{\underline{r}}_n^T)^T \\ + \frac{1}{8} \sigma_d^2 \rho_n^2 v_n^2 \Delta t^4 \dot{\underline{r}}_n \dot{\underline{r}}_n^T$$

$$Q_{13} = \frac{-1}{6} \rho_n v_n \sigma_d^2 \Delta t^3 \dot{\underline{r}}_n$$

$$Q_{22} = \sigma_a^2 \Delta t^2 I - \frac{1}{2} \sigma_a^2 \Delta t^3 \left[(2\underline{\Omega} \times I) + (2\underline{\Omega} \times I)^T \right] + \\ \sigma_a^2 \alpha_n \Delta t^3 (v_n^2 I + \dot{\underline{r}}_n \dot{\underline{r}}_n^T) + \frac{1}{4} \sigma_a^2 \Delta t^4 \left[(2\underline{\Omega} \times I) (2\underline{\Omega} \times I)^T - \right. \\ \left. \alpha_n (v_n^2 I + \dot{\underline{r}}_n \dot{\underline{r}}_n^T) (2\underline{\Omega} \times I)^T - \alpha_n (2\underline{\Omega} \times I) (v_n^2 I + \dot{\underline{r}}_n \dot{\underline{r}}_n^T) + \right. \\ \left. \alpha_n^2 (v_n^2 I + \dot{\underline{r}}_n \dot{\underline{r}}_n^T)^2 \right] + \frac{1}{3} \rho_n^2 v_n^2 \sigma_d^2 \Delta t^3 \dot{\underline{r}}_n \dot{\underline{r}}_n^T$$

$$Q_{23} = \frac{-1}{2} \rho_n v_n \sigma_d^2 \Delta t^2 \dot{\underline{r}}_n$$

$$Q_{33} = \sigma_d^2 \Delta t$$

$I = 3 \times 3$ Identity Matrix

Q_b = The user spacecraft's process noise time bias term

Q_b = The user spacecraft's process noise frequency bias term

Q_{bb} = The user spacecraft's process noise time bias/frequency bias coupling term

This formulation includes several terms that pertain to a modeled rotational force; these terms are underlined above. They were not computed in the GPSPAC software code because, during the design-code phase, the magnitude of these terms were judged to be insignificant by the design team. Consequently, the rotational force was not modeled in the GPSPAC software's version of the state-process-noise covariance matrix.

The Results of the Filter Parameter Changes

Heuberger used Landsat-4 data and ONPAC to analyze the effect on various navigation solutions by invoking the option to reduce the integration step size, by invoking the option to expand the state transition matrix Φ and by invoking the option to "tune" the state-process-noise covariance matrix Q_n . He discovered that by incorporating these changes before a simulated run, the simulated GPSPAC fluctuations were reduced considerably. Consequently, he recommended that these changes should be incorporated into the GPSPAC Kalman Filter software. For a detailed explanation of his results, see his paper entitled, "The Landsat-4/GPS Experiment Final Report".

A follow-up study was done with Landsat-5 data to test Heuberger's results and to reinforce his recommendations. This was accomplished by studying 2 specific arcs from the Landsat-5 data collection and by using ONPAC to invoke the same filter parameter options discussed above. These results, which concur with Heuberger's, are presented below in tabular and graphical form; also, a description of the filter parameters invoked is provided.

TABLE 1
GSTDN DEFINITIVE EPHEMERIS MAXIMUM ERRORS
OVER SELECTED 10-HOUR DATA ARCS

<u>Arc #</u>	<u>Start Time</u>	<u>Position (m)</u>	<u>Velocity (cm/sec)</u>
1	June 12, 1984, 05 ^h	48.7	4.2
2	July 24, 1985, 03 ^h	40.4	3.3

In Table 1 the two selected 10-hour data arcs are defined by their start dates and times. Furthermore, the maximum position/velocity errors of the GSTDN definitive ephemeris are given over each of the 10-hour data arcs. The maximum position/velocity errors were obtained by performing orbit fits over 24 to 32-hour tracking arcs with some overlap between successive arcs. The comparison of the two sets of GSTDN

definitive ephemeris over the common time span gives one a measure of the consistency between the two orbit solutions. It was assumed that the maximum error in position (velocity) over the two definitive arcs was less than the maximum position (velocity) difference in the overlap if the RMS of the USB range (range-rate) residuals from the two least squares fit was small (i.e. if the data fits were good).

TABLE 2
GPSPAC vs. ONPAC NAVIGATION ACCURACY

Arc #	Filter Options			Ephemeris Differences			
	h(sec)	Geopotential terms in Φ	σ^2 (m^2/sec^4)	Position(m)		Velocity(cm/sec)	
				MAX	RMS	MAX	RMS
1*	3.0	No	10^{-8}	720	268	184	43
1	1.0	No	10^{-8}	625	170	70	22
1	1.0	Yes	10^{-8}	526	165	65	22
1	1.0	Yes	10^{-6}	466	160	65	21
2*	3.0	No	10^{-8}	539	128	83	19
2	1.0	No	10^{-8}	346	102	63	15
2	1.0	Yes	10^{-8}	288	88	63	14
2	1.0	Yes	10^{-6}	238	83	57	12

*GPSPAC Solution

In Table 2, the ONPAC results from invoking the various filter parameter changes are summarized. The GSTDN definitive ephemeris was compared with the navigation solutions from GPSPAC as well as the navigation solutions from ONPAC. The runs were compared during the last 6 hours of each data arc to decrease the length of time required for ONPAC to process the navigation solutions. Moreover, the maximum position/velocity differences and their corresponding RMS for each one of the filter parameter changes invoked are given for one to analyze and to compare the effect on each navigation solution. A plot of GPSPAC/GSTDN definitive

position differences over the last 6 hours of arc #1 is shown in Figure 8 and the NDS visibility for this period is plotted in Figure 9. Similarly, the corresponding plots over the last 6 hours of arc #2 are shown in Figures 10 and 11.

By comparing the graphs of the GPSPAC/GSTDN definitive position differences, Figures 8 and 10, with the graphs of the NDS visibility Figures 9 and 11, one concludes that the GPSPAC fluctuations are large due to state error growth during periods of prolonged propagation. Also, the fact that GPSPAC uses a simple integration scheme—modified Euler with one derivate evaluation per step—definitely increases the risk of incurring large error growth during poor SV visibility. However, just by reducing the step size from 3 seconds to 1 second, the error growth became significantly bounded. For the comparison using arc #1, refer to Figure 8, the GPSPAC/GSTDN definitive position differences; Figure 12, the ONPAC/GSTDN definitive position differences with no changes and Figure 13, the ONPAC/GSTDN definitive position differences with 1.0 step size. Likewise, Figures 10, 16, and 17 give the corresponding comparison for arc #2.

A previous section of the paper explains the fact that the design plans for the state transition matrix, Φ , included the modeled geopotential acceleration terms, yet, for reasons unknown, these terms were not included in the code. However, ONPAC offers the capability of including the gravity acceleration terms as a filter parameter option. So this option was exercised over both data arcs and Table 2 shows just how much the maximum position/velocity differences decreased by expanding Φ to include the geopotential acceleration terms. Figures 14 and 18 illustrate the reduction seen in the GPSPAC fluctuations by using a smaller step size, 1.0 second and by using an expanded Φ which included the geopotential acceleration terms for each time span.

A process called "tuning the filter" was exercised over the 2 arcs in order to compensate for the GPSPAC Kalman Filter's underestimate of the true error during periods of poor SV visibility. To "tune the filter" one has to adjust the position-velocity components of the state-process-noise covariance matrix, Q_n , which are proportional to the date base constant σ_a^2 —the unmodeled acceleration variance; so by changing σ_a^2 accordingly, the filter is kept from diverging and hence, it produces a better estimate of the true error during periods of prolonged propagation due to poor SV visibility. The constant was increased from $10^{-8} \text{m}^2/\text{sec}^4$ to $10^{-6} \text{m}^2/\text{sec}^4$ (see Table 2). This filter parameter adjustment improved the error dynamics model significantly. Figures 15 and 19 show the ONPAC/GSTDN definitive position differences with all three filter parameter options invoked: the 1.0 step size reduction, the expanded Φ matrix which included the geopotential acceleration terms, and the tuned filter result from increasing σ_a^2 .

ORIGINAL PAGE IS
OF POOR QUALITY

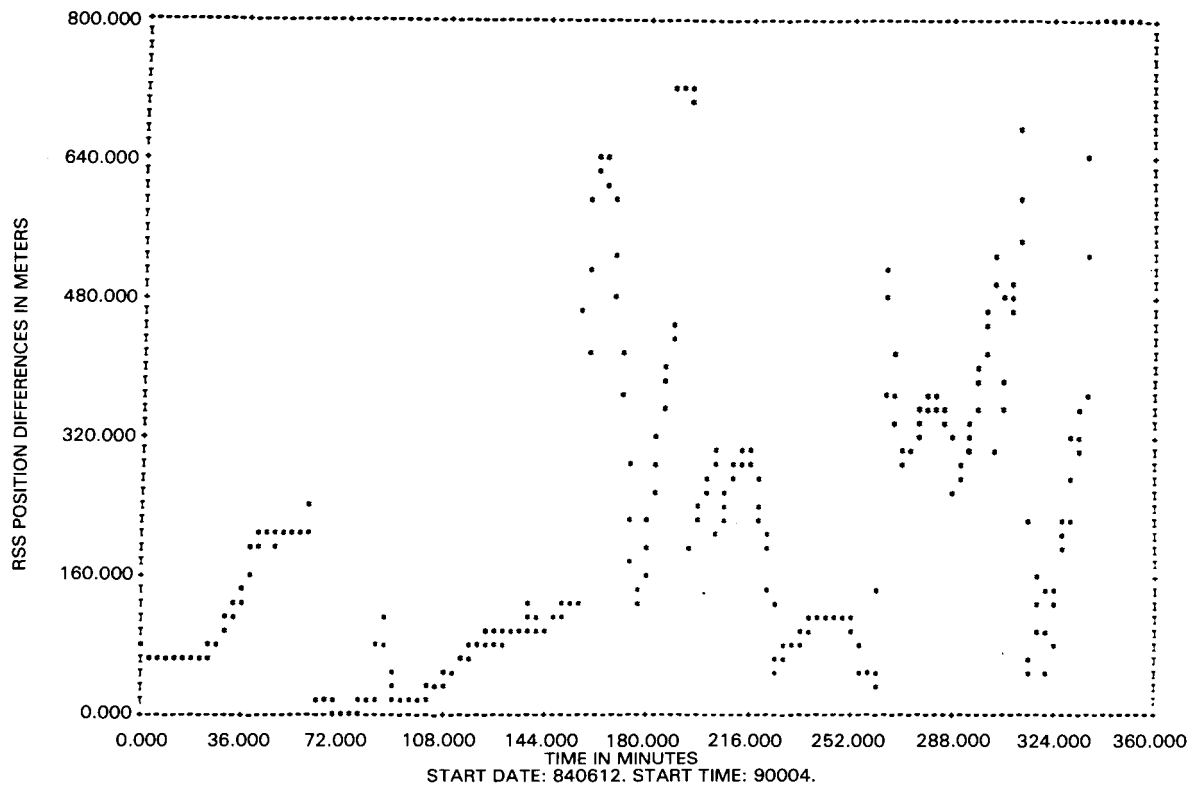


Figure 8. GPSPAC/GSTDN Definitive Position Differences - Arc #1

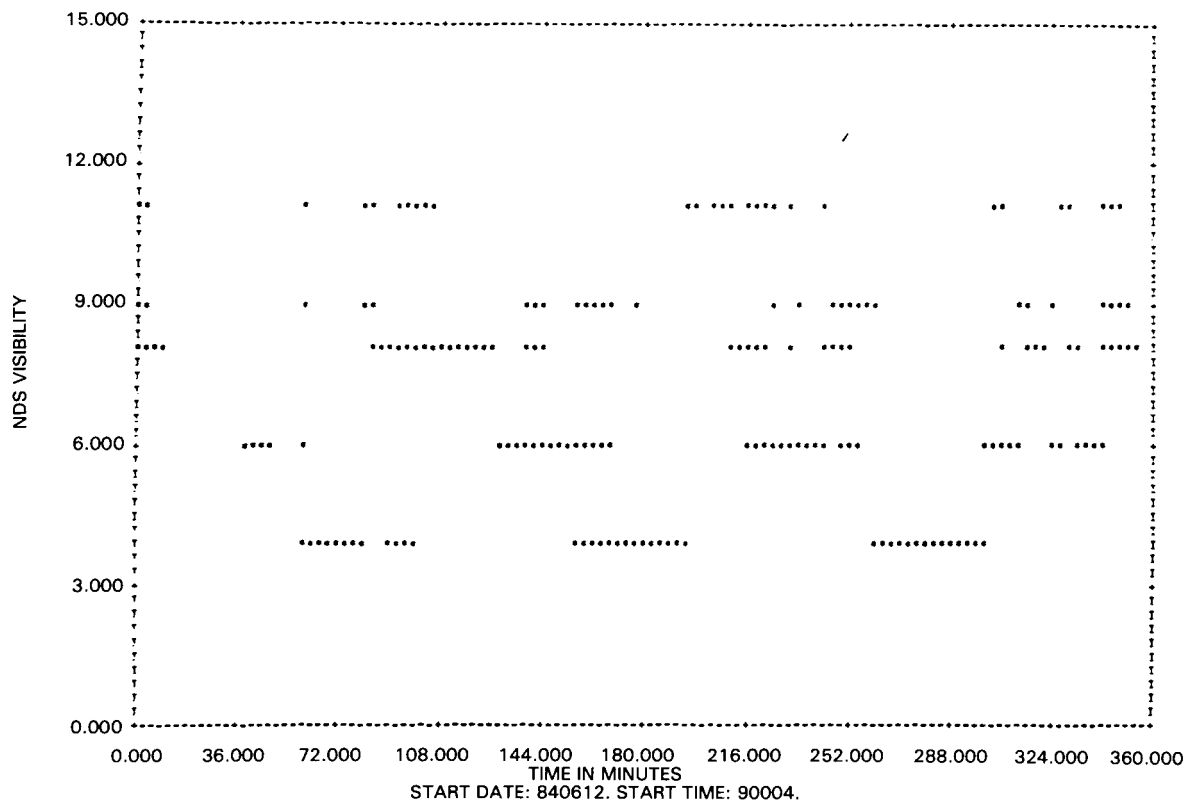


Figure 9. NDS Visibility to Landsat-5 - Arc #1

ORIGINAL PAGE IS
OF POOR QUALITY

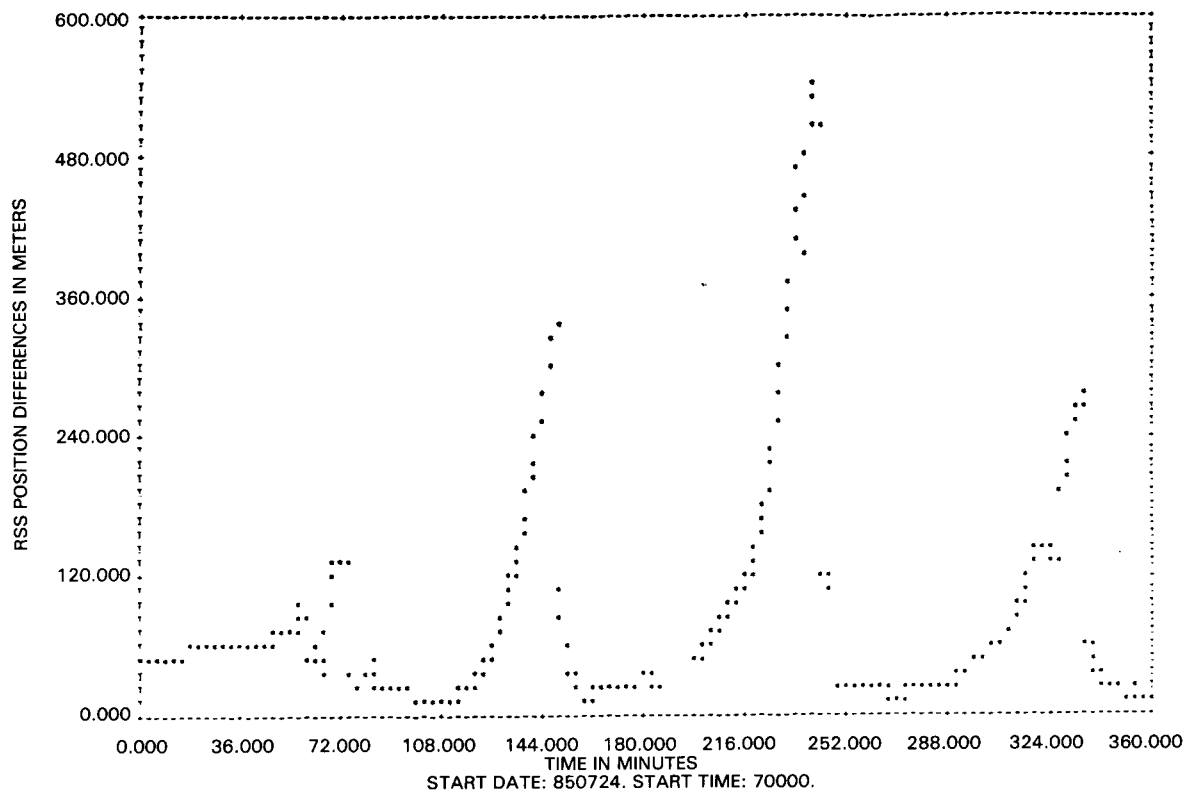


Figure 10. GPSPAC/GSTDN Definitive Position Differences - Arc #2

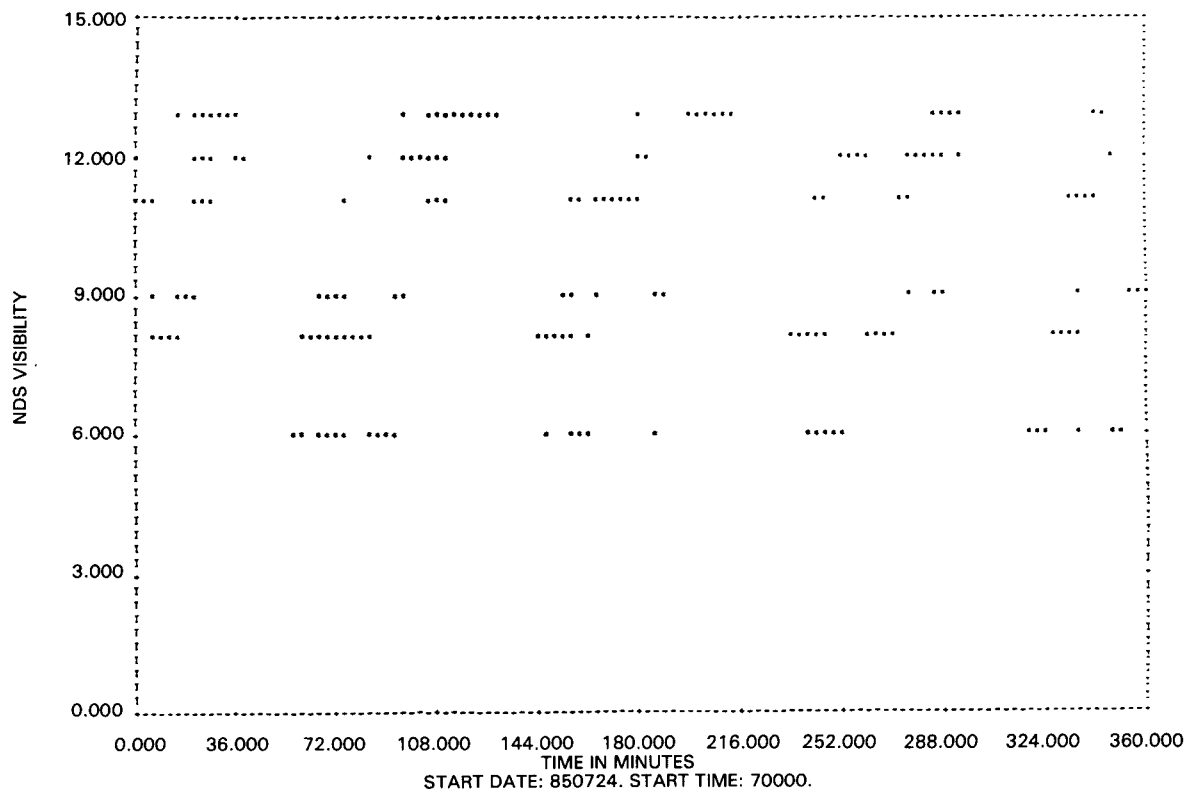


Figure 11. NDS Visibility to Landsat-5 - Arc #2

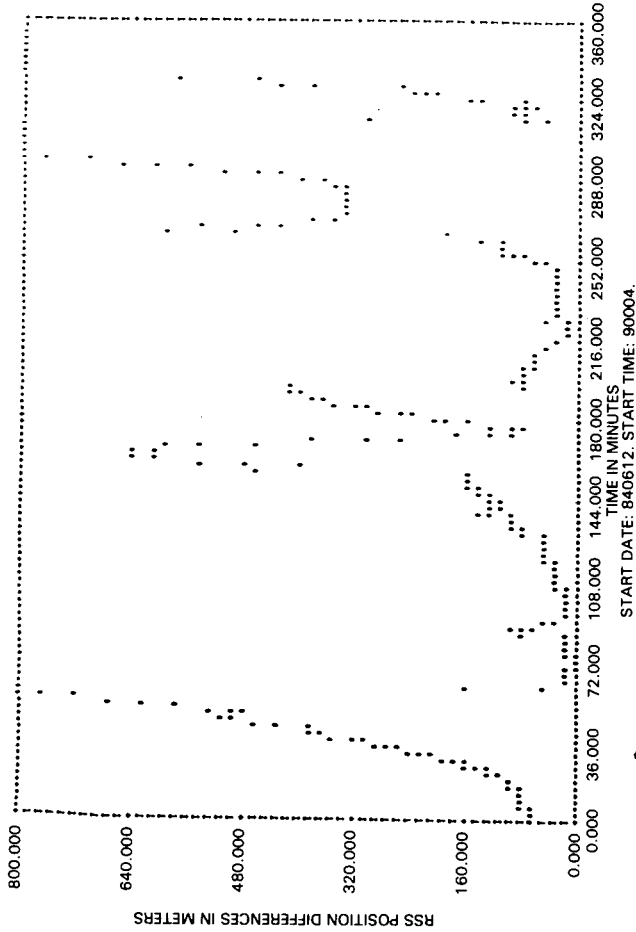


Figure 12. ONPAC/GSTDN Definitive Position Differences
- Arc #1 (No changes)

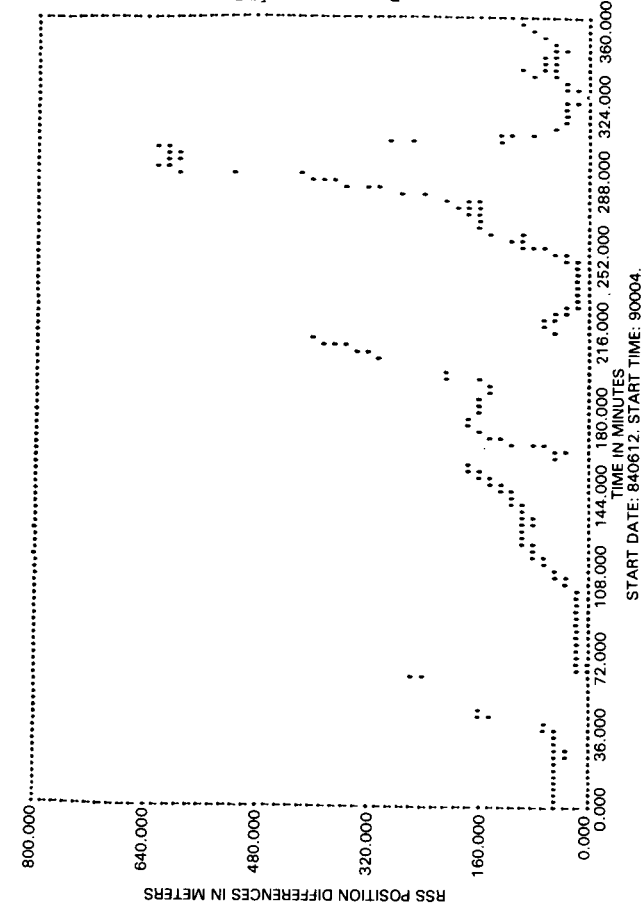


Figure 13. ONPAC/GSTDN Definitive Position Differences
- Arc #1 (h + 1 second)

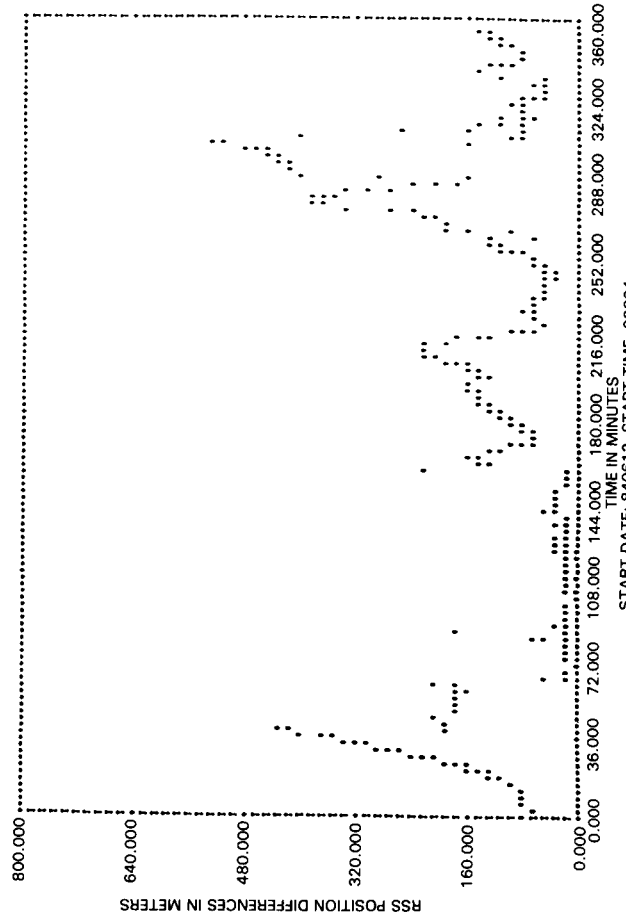


Figure 14. ONPAC/GSTDN Definitive Position Differences
(h + 1 second, Geopotential terms in Φ)

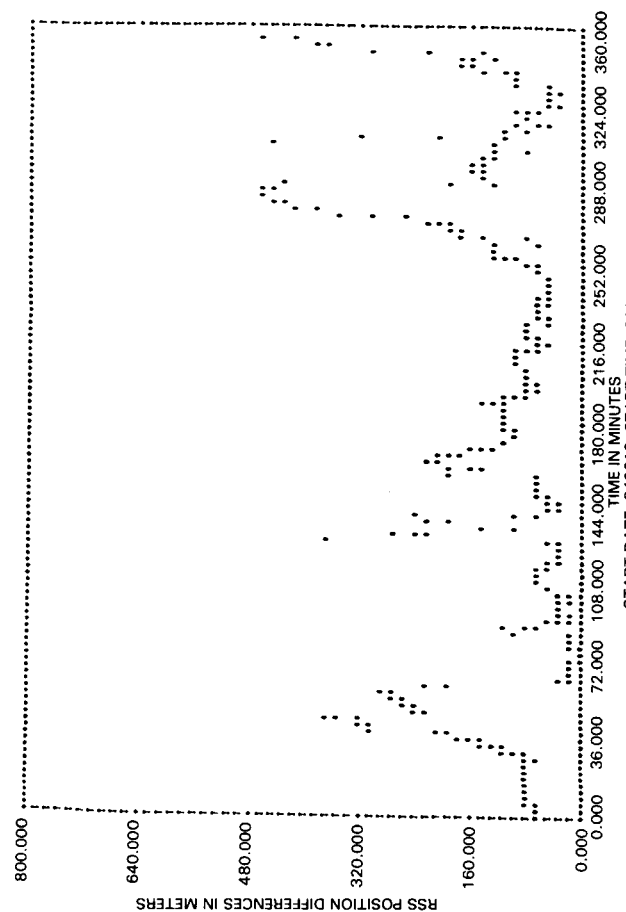


Figure 15. ONPAC/GSTDN Definitive Position Differences
- Arc #1 (h + 1 second, Geopotential terms
in $\Phi, \sigma_a^2 = 10^{-6} \text{ m}^2/\text{sec}^4$)

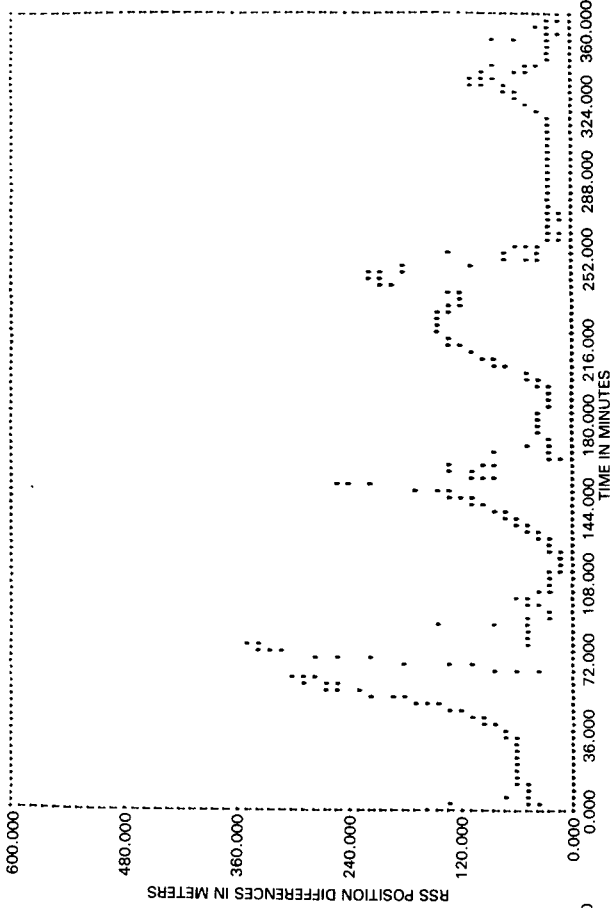


Figure 16. ONPAC/GSTDN Definitive Position Differences
- Arc #2 (No changes)

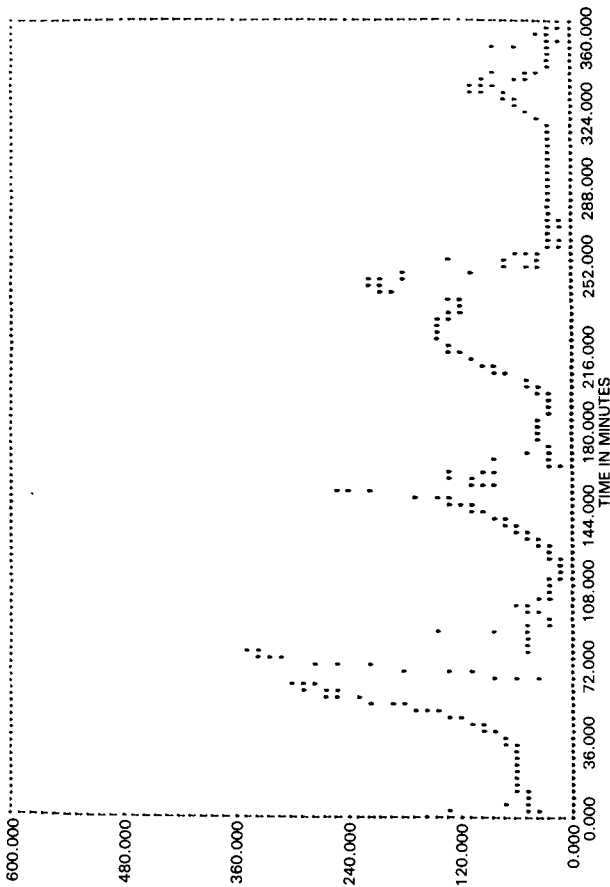


Figure 17. ONPAC/GSTDN Definitive Position Differences
- Arc #2 (h + 1 second)

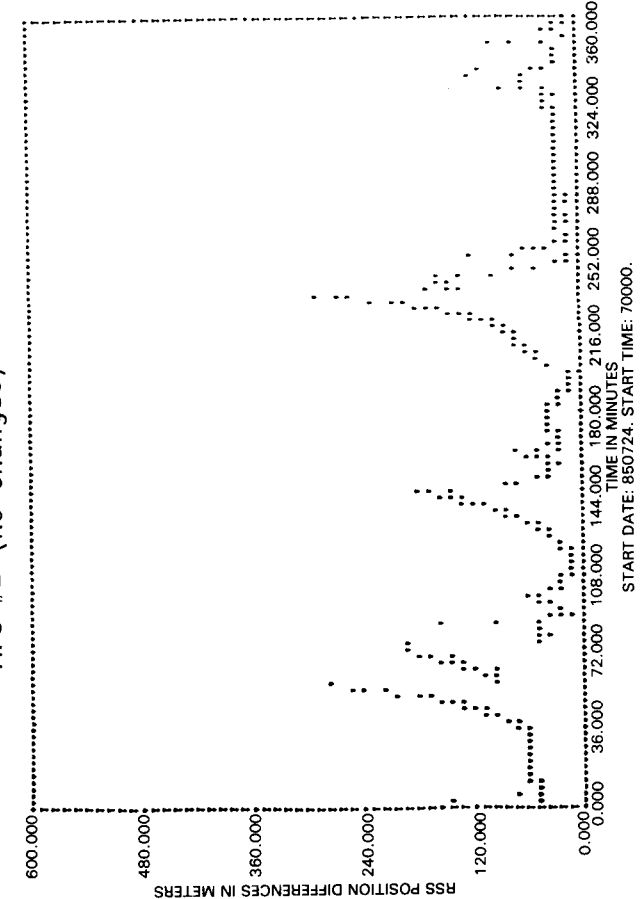


Figure 18. ONPAC/GSTDN Definitive Position Differences
- Arc #2 (h + 1 second, Geopotential terms
in Φ)

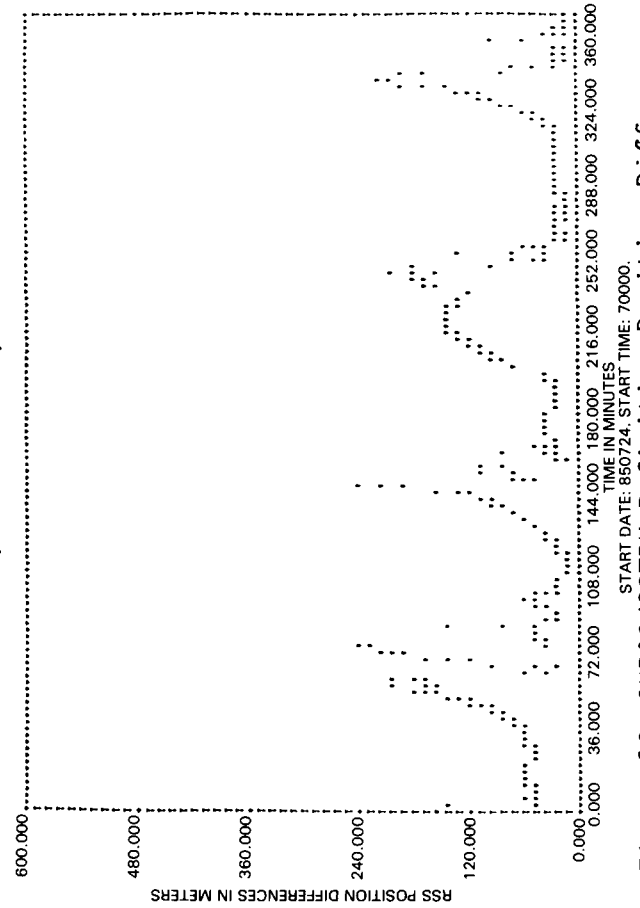


Figure 19. ONPAC/GSTDN Definitive Position Differences
- Arc #2 (h + 1 second, Geopotential terms
in $\sigma_a^2 = 10^{-6} \text{ m}^2/\text{sec}^4$)

The Implications of the Steps Taken to Reduce the Simulated GPSPAC Fluctuations

The comparison of the GPSPAC navigation design with the code proved to be a step in the right direction for two reasons. First of all, it helped us detect a couple of problems that occurred in the way the EKF state-error covariance matrix was designed and implemented—namely, the Ξ and Q_n design-code differences. Secondly, although the magnitude of the rotational force terms of the Q_n matrix were indeed insignificant (proven by hand calculations), expanding Ξ to include the geopotential acceleration terms did help to reduce the simulated GPSPAC fluctuations considerably (this result is shown in the section entitled, "The Results of the Filter Parameter Changes").

In addition to the expanded Ξ matrix, two other filter parameter options invoked during a ONPAC simulated run also helped to reduce the simulated GPSPAC fluctuations: decreasing the integration step size and increasing σ_a^2 to tune the filter. Because these results were shown in a follow-up study using Landsat-5 data, Heuberger's software recommendations are reinforced and are very easy to accommodate—the step size can easily be reduced to 1.0 second; the Ξ matrix can easily be expanded to include the geopotential acceleration terms; and the Q_n matrix can easily be tuned by just changing the data base constant, σ_a^2 .

5.0 CONCLUSIONS

A GPSPAC/Landsat-D Interface (GLI) ground support system was built to validate the performance and to calibrate the accuracy of the experimental navigation package, GPSPAC, flown on the Landsat-4 and 5 spacecraft. Although the GLI system has operated successfully to give the orbit information needed to validate the GPSPAC, it also detected the following two anomalies. The first problem which pertains to the ONPAC system is that the ONPAC orbit propagator is inconsistent with the orbit propagation model of GPSPAC. The second problem, which pertains to the pre-operational phase of GPS, is that the GPSPAC position (velocity) difference fluctuations are large whenever the user spacecraft is forced to propagate its own orbit because of poor SV visibility. Two attempts were made to resolve the ONPAC inconsistencies: (1) comparing the GPSPAC navigation code against the supposedly equivalent ONPAC code and modifying the non-conforming routines. (2) hand-calculating various filter parameters (to see if these answers matched the answers given by ONPAC). However, neither one of them helped; but, it turned out that by invoking the same

filter parameter options which were used to reduce the simulated GPSPAC fluctuations also helped to reduce the ONPAC inconsistencies. The steps taken to reduce the simulated GPSPAC fluctuations were discovered by Heuberger. He recommended that the following changes should be made to the GPSPAC software: (1) reducing the integration step size from 3.0 seconds to 1.0 second, (2) expanding the state transition matrix to include the geopotential acceleration terms, (3) increasing the unmodeled acceleration variance to tune the Extended Kalman Filter. A follow-up study using ONPAC and Landsat-5 data was done to test Heuberger's recommended changes. The results of the study concurred with his; therefore, his recommendations are reinforced.

Theoretically, several possible software changes could be made to ONPAC to reduce the simulated GPSPAC fluctuations, such as upgrading the numerical integration scheme to a Runge-Kutta integration scheme. But, the software would have to be re-designed, re-built, and re-tested which would be costly. However, the recommendations mentioned above can be easily incorporated in the GPSPAC software thereby making them the preferred solution.

The future of GPSPAC remains to be seen since it is uncertain if Landsat or any other spacecraft, for that matter, will ever fly another GPS navigation package. However, since August 1986, the Systems Development Branch was finished with the project in terms of collecting, processing, and analyzing GPSPAC data; we will always keep a consolidated collection of good GPSPAC continuous data arcs from the Landsat-4 and 5 spacecraft for future independent studies of autonomous onboard navigation systems--for example, there is speculation that GPS may be used on Space Station and we will remain as a point of contact for obtaining various information pertaining to the GPSPAC/Landsat-D Interface ground support system.

ACKNOWLEDGMENT

I would like to thank Mr. Howard Heuberger of Johns Hopkins Applied Physics Laboratory for the time, effort, and assistance that he gave to me on the Landsat/Global Positioning System project.

REFERENCES

1. Sielski, H. M. and Dunham, J. B., "GPSPAC/Landsat-D Interface (GLI) System User's Guide", Systems Technology Laboratory Series, STL/882/002, March 1982, pp. 1-3, 6-1.
2. Uyeminami, R. T., "Navigation Filter Mechanization for a Spaceborne GPS User", Proc. IEEE Position Location and Navigation Symposium, November 1978, pp. 330.
3. Dunham, J. B., "Mathematical Specifications of the Onboard Navigation Package (ONPAC) Simulator (Revision 1)", Computer Sciences Corporation, CSC/SD-8116028, February 1981, pp. 3-13, 5-1.
4. Heuberger, H. S., "Landsat-4/GPS Experiment Final Report", NASA/Goddard Space Flight Center, December 1983, pp. 34-40.